Increased Mortality Rate and Not Impaired Ribosomal Biogenesis is Responsible for Proliferative Defect in Dyskeratosis Congenita Cell Lines

Lorenzo Montanaro, Alessandra Chillà, Davide Trerè, Annalisa Pession, Marzia Govoni, Pier Luigi Tazzari,* and Massimo Derenzini

Dipartimento di Patologia Sperimentale, Università degli Studi di Bologna, Bologna, Italy; *Centro Trasfusionale, Policlinico S. Orsola – Malpighi, Bologna, Italy

X-linked dyskeratosis congenita is a rare inherited disorder mainly characterized by progressive changes in proliferating epidermal, mucosal, and bone marrow tissues that commonly emerge after 10 y of life. It is caused by mutations of the *DKC1* gene, which codes for dyskerin, a protein that may play a role in ribosomal biogenesis. In order to verify whether the defects of proliferating tissues observed in dyskeratosis congenita are due to an altered ribosome synthesis, we studied ribosomal biogenesis in relation to cell proliferation in two lymphoblastoid cell lines from dyskeratosis congenita patients and in one control line. We observed that in the dyskeratosis congenita cell lines the rRNA transcription and maturation and proliferative capability remained unimpaired. Increasing the number of cell cycles, however, leads to a steep rise in the apoptotic fraction of dyskeratosis congenita cells, which is not observed in controls. These findings demonstrate that whereas dyskeratosis congenita cell lines do not display proliferation defects, they do show progressively increasing levels of apoptosis in relation to the number of cell divisions. This concept is consistent with (i) the delayed onset of dyskeratosis congenita proliferating-tissue defects, which do not emerge during embrional development as would be expected with ribosomal biogenesis alterations, and (ii) with the increasing severity of the proliferating-tissue defects over time. ***Key words: apoptosis/cell nucleolus/ribosomal RNA/Zinsser–Cole–Engman syndrome. J Invest Dermatol 118:193–198, 2002***

X-linked dyskeratosis congenita (DKC, OMIM# 305000) is a rare inherited disorder, characterized by the triad of reticulate skin pigmentation, nail dystrophy, and mucosal leucoplakia (Zinesser, 1906; Engmann, 1926; Cole *et al*, 1930). The main noncutaneous abnormality is a progressive bone marrow failure that occurs in over 80% of patients and represents the major cause of premature death (Dokal, 1996; Knight *et al*, 1998). Considering these clinical features, it is clear that tissues that need continual renewal are most affected by the genetic lesion underlying the disorder.

DKC is caused by mutations of the *DKC1* gene (Heiss *et al*, 1998; Knight *et al*, 1999), which codes for a protein localized in the nucleolus called dyskerin (Heiss *et al*, 1999). Dyskerin is homolog to two eukaryotic proteins: the rat Nap57 and the Cbf5p of *Saccaromyces cerevisiae* (Knight *et al*, 1999). Nap57 is associated with the nucleolar peptide Nopp140, and this complex contributes to the maturation of rRNA and allows the shuttling of the newly synthesized ribosomal proteins and intermediate precursors of the ribosomal subunits (Meier and Blobel, 1992; Meier and Blobel, 1994). Cbf5p is a phosphoprotein that during interphase localizes within the nucleolus and contributes to ribosomal biogenesis (Cadwell *et al*, 1997). Dyskerin also interacts with the H/ACA domain present at the 3′ end of the RNA of telomerase. In DKC lymphoblasts and fibroblasts, the telomerase activity is lower and the telomeres are shorter than in nonaffected cells (Mitchell *et al*, 1999). The proliferative alterations observed in DKC could thus be ascribed either to a defect in ribosomal biogenesis or to an altered activity of telomerase.

We set out to investigate whether the proliferative alterations of DKC are indeed caused by a defect in rRNA transcription and maturation. For this purpose, we employed three lymphoblastoid cell lines: two derived from two brothers affected by DKC, and a control cell line derived from a nonaffected individual. As parameters of ribosomal biogenesis rRNA synthesis and maturation were measured by [^{3}H]uridine incorporation and nuclear rRNA fractionating. The ultrastructural features of the nucleolus and the nucleolar size after silver staining were also evaluated. The proliferation rate was measured in the three cell lines by evaluating the population doubling time (DT) and by [^{3}H]thymidine incorporation. Surprisingly, the DKC cells showed greater ribosomal biogenesis, with normal maturation processes, larger nucleoli, and higher DNA synthesis than the control cell line. In contrast, and in agreement with previous data (Dokal *et al*, 1992), the population DT of DKC cell lines was longer than that of control cells. To investigate whether the longer DT of DKC cells might be caused by a greater cell mortality we evaluated the

Manuscript received May 10, 2001; revised September 20, 2001; accepted for publication October 8, 2001.

Reprint requests to: Dr. Lorenzo Montanaro, Dipartimento di Patologia Sperimentale, via S. Giacomo 14, 40126 Bologna, Italy. Email: montana@med.unibo.it

Abbreviations: DKC, dyskeratosis congenita; DT, doubling time; NOR, nucleolar organizer regions.

0022-202X/01/$15.00 · Copyright © 2002 by The Society for Investigative Dermatology, Inc.

percentage of dead cells both by Trypan blue exclusion test and by flow cytometry. We found that in both DKC cell lines the mortality rate progressively increased over time (up to 3-fold). By contrast, in the control line the mortality rate remained quite constant. Our findings therefore indicate that the reduced growth rate of DKC cell lines is not due to an impaired ribosomal biogenesis but to a progressive increase in cell death.

MATERIALS AND METHODS

Cell cultures Three cell lines (GM3193, GM3194, GM130c) of lymphocytes immortalized by Epstein–Barr virus, from Coriell Cell Repositories (Coriell Institute for Medical Research, Camden, NJ), were used. The GM3193 and GM3194 cell lines derive from two brothers affected by DKC and harbor an A→G missense mutation in the *DKC1* gene in position 196 (T66A) (Knight *et al*, 1999). The control GM130c cell line derives from a nonaffected individual.

The cells were grown as a suspension culture in RPMI 1640, 20% heat-inactivated fetal bovine serum, 0.5% nonessential amino acids, 100 U per ml penicillin, 100 μg per ml streptomycin, and 1% L-glutamine. The cells were incubated at 37°C in a humidified atmosphere of 5% CO_2–95% air. The population DTs were obtained by growing inocula of 5×10^4 cells in 24-multiwell plate wells, and counting the cells at 24 h intervals in triplicate, according to the method of Patterson (1979).

For the weekly evaluations, an aliquot of each cell line, which was frozen soon after its arrival, was thawed and cultured as described above. Each week, the cells needed for mortality and proliferation rate evaluations were taken from each culture.

Evaluation of nucleolar size by silver staining of nucleolar organizer region (NOR) associated proteins Cells were collected from each cell line by centrifugation. Pellets were treated with 0.075 M KCl at 37°C for 1 h and fixed in 70% ethanol for 30 min at 4°C. After several changes of the same solution, the cells were dropped onto clean glass slides, postfixed for 30 min in 70% ethanol, rehydrated, and stained with silver. AgNOR protein staining was carried out according to Ploton *et al* (1986), using a solution of 1 vol of 2% gelatine and 1% formic acid and 2 vol of 50% silver nitrate for 13 min at 37°C. After washings, the slides were dehydrated and mounted in a synthetic medium. For each sample, the AgNOR protein area within 100 nuclei was measured using a specific program (Image-Pro Plus 3.02, Media Cybernetics, Silver Spring, MD) of a computer-assisted image analysis system. The system consisted of a 3 CCD color video camera (KY F55B, JVC) mounted on a Leitz light microscope and connected with a Pentium II PC (Pana Sync S70, Panasonic). The mean value and the standard deviation in square microns were automatically obtained for each case.

Transmission electron microscopy analysis Cells were collected from each cell line and fixed in paraformaldehyde, postfixed in osmium tetroxide, dehydrated in ethanol, and embedded in Araldite. Thin sections, double stained with uranyl acetate and lead citrate, were examined with a Philips 410T.

RNA and DNA synthesis evaluation [^{3}H]uridine (2.5 μCi per ml) was added for the last 30 min of culture. Thereafter, unlabeled uridine (1 mM in culture medium) was added and cells were harvested by centrifugation at 1200*g* for 5 min. Nuclei were extracted in TKM buffer (10 mM Tris–HCl pH 7.4, 10 mM KCl, 3 mM $MgCl_2$) containing 0.1% Triton-X 100 and washed with 0.25 M sucrose in TKM buffer at 4°C. Nuclei were then suspended in Tris-acetate 0.1 M pH 5.2, and the samples were used for total RNA determination and stepwise extraction with phenol at 4°C and 50°C. Each extraction step was repeated twice, and the samples obtained were joined before radioactivity assessment. The two nuclear fractions, 4°C and 50°C, corresponded to mature and precursor rRNA, respectively (Dabeva *et al*, 1978; Derenzini *et al*, 1987). RNA synthesis was measured considering the ratio between the radioactivity and the 260 nm absorbance for each fraction. To obtain a qualitative and quantitative control, the extracted 4°C and 50°C rRNA fractions were size separated on a 1% agarose gel and stained with ethidium bromide. An amount of RNA corresponding to a radioactivity of 2000 DPM and 6000 DPM was loaded for the 4°C and 50°C fraction, respectively.

[^{3}H]thymidine (1 μCi per ml) was added to the cells for the last hour of culture; cells were counted in triplicate after Trypan blue staining and collected, and DNA was extracted at 70°C in 7% perchloric acid (Derenzini *et al*, 1987). Radioactivity of samples was measured and expressed as a function of the number of alive cells.

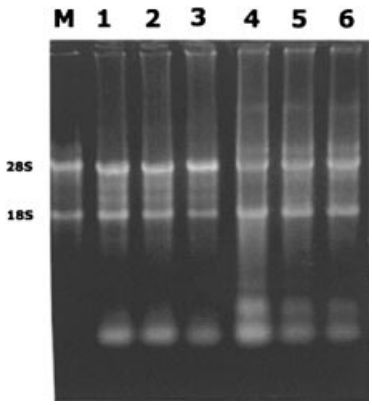

Figure 1. Nuclear RNA fractionating. 4°C and 50°C extracted rRNA fractions size separated on a 1% agarose gel and ethidium bromide stained. M, human 28S and 18S rRNA. *Lanes 1, 2, 3*: 4°C extracted RNA corresponding to a radioactivity of 2000 DPM from GM130c (control), GM3193 (DKC) and GM3194 (DKC), respectively. *Lanes 4, 5, 6*: 50°C extracted RNA corresponding to a radioactivity of 6000 DPM from GM130c (control), GM3193 (DKC), and GM3194 (DKC), respectively.

Cytofluorimetric analysis For flow cytometry analysis, cells were collected by centrifugation, fixed in 70% ethanol, and stained using the DNA-PREP Stain Kit (Coulter, Miami, FL) following the manufacturer's instructions. The analysis was performed using a Coulter Epics XL (Coulter). Apoptotic cells were identified and measured on the propidium iodide fluorescence histogram as a hypodiploid peak as described previously (Nicoletti *et al*, 1991).

Statistical analysis Differences between groups were evaluated by Student's *t* test. A p-value ≤ 0.05 was considered significant.

RESULTS

The lymphoblastoid cell lines GM130c, GM3193, and GM3194 were cultivated for 3 d immediately after arrival from the Coriell Cell Repository. Then, for each line, several aliquots of cells were stored in liquid nitrogen; other cells were grown in order to evaluate their ribosomal biogenesis, the size and morphology of nucleoli, and proliferative activity.

The rRNA synthesis in the three cell lines was evaluated by measuring the radioactivity of the RNA extracted from nuclei after 30 min of [^{3}H]uridine incorporation. In this method, the nuclear rRNA is extracted first at 4°C, isolating the nucleoplasmic, mature rRNA, and then at 50°C, isolating the nucleolar precursor rRNA (Dabeva *et al*, 1978; Derenzini *et al*, 1987). The quality of the extracted RNA was confirmed by agarose gel electrophoresis and ethidium bromide staining. **Figure 1** shows that 4°C fractions (*lanes 1, 2, 3*) are constituted mainly by 28S and 18S rRNA mature subunits, whereas the 50°C fractions (*lanes 4, 5, 6*) contain lower quantities of 28S and 18S rRNA and are enriched with higher molecular weight precursor rRNA. The radioactivity of the 50°C fraction loaded in the gel was three times greater than that of the 4°C fraction because the lower quantity was not sufficient to clearly detect rRNA by ethidium staining. The intensity of the 28S and 18S bands in the 50°C fractions was lower (by approximately one-half) than in the 4°C fractions. These results are in line with those described by Dabeva and coworkers who originally described the extraction method and demonstrate that incorporated radioactivity in the 50°C fraction has to be mainly ascribed to precursor molecules. The data obtained give information both on rRNA maturation and rRNA transcription. In the 4°C fraction and especially in the 50°C fraction the radioactivity of the DKC cell lines was clearly greater than in the control line ($p < 0.05$ and $p < 0.01$, respectively; **Table I**). The percentage of radioactivity

Table I. Cell proliferation and nucleolar function in the studied cell lines

	DT (h)[a]	Nucleolar area (μm^2)[a]	[^{3}H]thymidine incorporation (DPM per alive cell $\times 10^{-2}$)[a]	[^{3}H]uridine incorporation and RNA fractionating (DPM per μg RNA)[ab]		Percentage of alive cells[a]
				4°C	50°C	
GM130c	23 ± 6	6.2 ± 2.7	2.3 ± 0.1	557.9 ± 46.7 (29%)	1365.1 ± 215.8 (71%)	91 ± 6.4%
GM3193	75 ± 12*	10.8 ± 5.8*	4.7 ± 0.3*	698.6 ± 65.4* (20.6%)	2695.8 ± 184.1 (79.4%)	68 ± 11.2%*
GM3194	70 ± 4*	9.8 ± 5.8*	4.4 ± 0.2*	746.9 ± 56.2* (22.9%)	2515.5 ± 267.6 (77.1%)	70 ± 8.6%*

[a]Data are expressed as mean ± SD.
[b]The percentage of radioactivity incorporated is reported in parentheses.
*Significant difference ($p < 0.05$) *versus* control cell line (GM130c).

incorporated in the rRNA newly synthesized molecules found in the 4°C fraction was slightly lower in the DKC cell lines (20.6% and 22.9% for GM3193 and GM3194, respectively) than in the control line (29%).

Concerning the nucleolar size of the DKC and control cell lines, it was evaluated on silver-stained cytologic preparations by computer-assisted morphometric analysis. The mean nucleolar areas of the DKC GM3193 (10.8 ± 5.8 μm^2 mean ± SD) and GM3194 (9.8 ± 5.8 μm^2 mean ± SD) cell lines were found to be significantly greater than that of the control cell line (6.2 ± 2.7 μm^2 mean ± SD; $p < 0.01$; **Fig 2**, **Table I**).

Regarding the nucleolar morphology, the ultrastructural distribution of nucleolar components was evaluated on thin sections stained with uranyl acetate and lead citrate. The ribonucleoprotein components of the nucleoli of the three cell lines were organized in a very similar manner. In the two DKC cell lines, hypertrophied nucleoli with many fibrillar centers, surrounded by an evident dense fibrillar component, were present more frequently than in the control cell line (**Fig 3**).

Cell proliferation was initially evaluated as population DT, measured by counting the growing cells at 24 h intervals. The DKC cell lines were characterized by a DT of 75 ± 12 h (mean ± SD) for GM3193 and 70 ± 4 h (mean ± SD) for GM3194, whereas that of the GM130c control cell line was 23 ± 6 h (mean ± SD). As the morphology and size of the nucleoli and their functional activity were in clear contrast with the data on the DT of the three cell lines (the nucleolar size and the function are normally inversely related to cell DT) (Derenzini *et al*, 1998; 2000), we analyzed DNA synthesis standardized to an equal number of alive cells. The incorporation of [^{3}H]thymidine was significantly higher in the two DKC cell lines (4.7×10^{-2} DPM per cell for GM3193 and 4.4×10^{-2} DPM per cell for GM3194) than in the control line (2.3×10^{-2} DPM per cell; $p < 0.01$), indicating that the DKC cell lines have higher proliferative activity than the control.

This initial group of experiments had demonstrated that the slower expansion of the DKC cell lines was not due to a reduction of ribosomal biogenesis or to reduced proliferative activity. To try to explain the lower DT of the DKC cell lines, in a successive group of experiments we evaluated the entity of cell death over a period of 4 wk. For this purpose, an aliquot of each cell line originally stored in liquid nitrogen was thawed and cultivated to evaluate the weekly variations of the following parameters: (i) percentage of vital cells after Trypan blue staining and light microscopy; (ii) percentage of dead cells as evaluated by cytofluorimetric analysis of the hypodiploid peak after propidium iodide staining; (iii) the entity of [^{3}H]thymidine incorporation and the population DT.

The percentage of nonvital cells evaluated by Trypan blue exclusion test increased considerably in the DKC GM3193 and GM3194 cell lines during the 4 wk, reaching values of 69% and 95%, respectively, at the end of the fourth week (**Table II**),

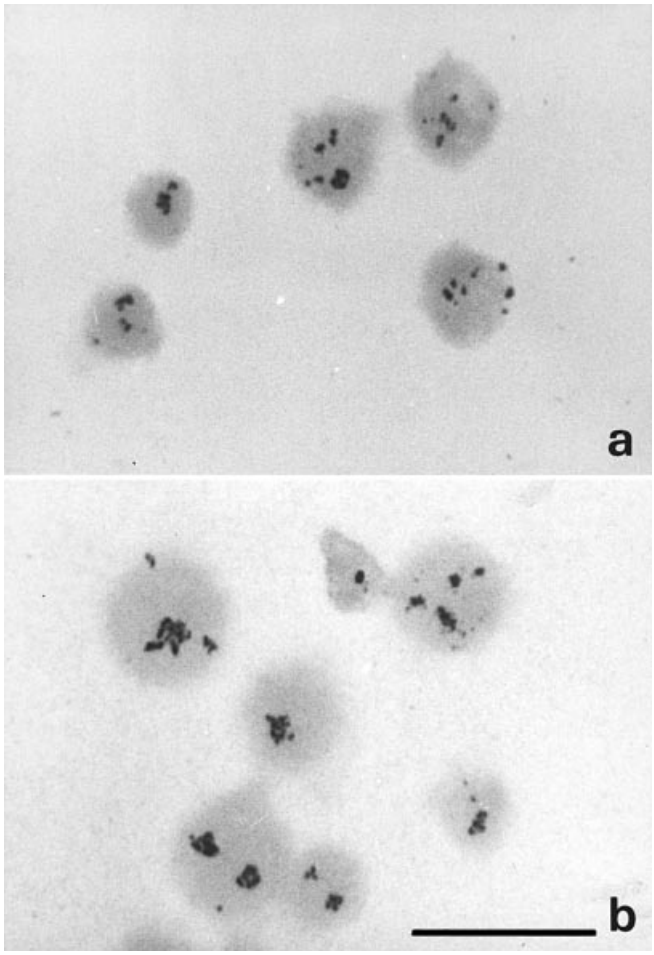

Figure 2. Evaluation of AgNOR area. Cytologic preparations from GM130c (control) (*a*) and GM3193 (DKC) (*b*) cell lines stained with silver for the selective visualization of AgNOR proteins. A higher amount of stained structures in the DKC line (mean area 10.8 ± 5.8 μm^2) than in control line (mean area 6.2 ± 2.7 μm^2) is evident. *Bar*: 50 μm.

compared with 28% in the GM130c cell line ($p < 0.01$). These data were confirmed by cytofluorimetric evaluation, which showed a progressive increase of the hypodiploid peak in the DKC cell lines but a quite constant peak in the control line (**Fig 4**). The incorporation of [^{3}H]thymidine standardized for an equal number of alive cells was always higher in the DKC cell lines than in the control line, and the ratio between the incorporated radioactivity

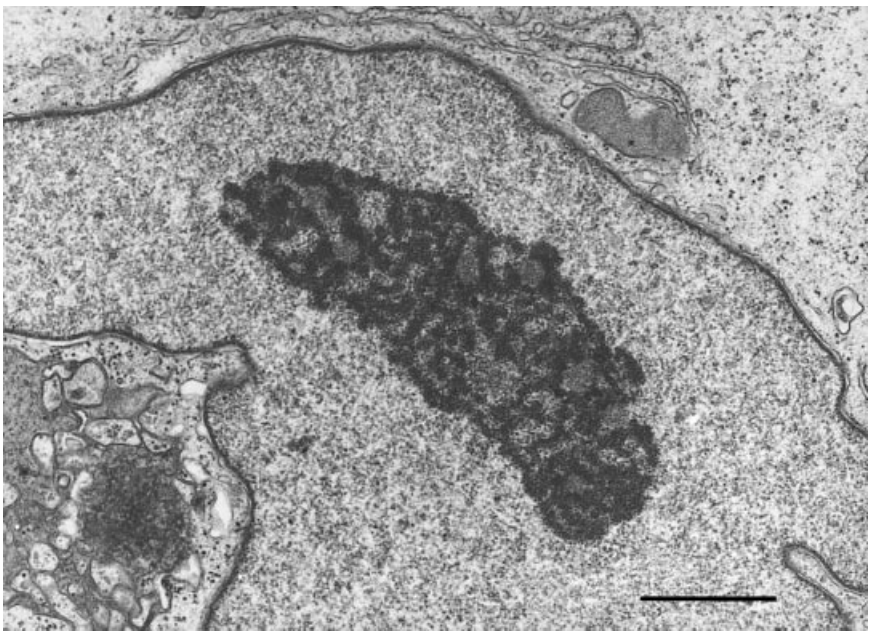

Figure 3. Ultrastructural features of nucleolus in a DKC cell line. Thin section of a GM3193 cell. Numerous fibrillar centers surrounded by dense fibrillar component are evident in the enlarged nucleolus. These features are characteristic of an intense rRNA synthesis. Uranium and lead staining; *bar*: 1 μm.

Table II. Cell death and proliferation in the studied lines during 4 wk

		First week	Second week	Third week	Fourth week
Dead cell (%): mean ± SD	GM130c	19 ± 7	22 ± 5	26 ± 11	28 ± 11
	GM3193	20 ± 4	46 ± 4*	60 ± 12*	69 ± 5**
	GM3194	22 ± 5	16 ± 6	52 ± 9*	95 ± 9**
Cytofluorimetric hypodiploid peak (%)	GM130c	12.5	7.6	13.3	16.2
	GM3193	6.9	18.8	20.2	48.7
	GM3194	9.2	20.7	29	65.4
[^{3}H]thymidine incorporation (DPM × 10^{-3} per alive cell): mean ± SD	GM130c	4.1 ± 0.9	4.5 ± 0.8	2.4 ± 0.3	3.8 ± 1
	GM3193	7.3 ± 2	7.4 ± 1.1*	6 ± 0.2**	8.6 ± 2.5*
	GM3194	9.6 ± 0.3**	9.4 ± 3.3	3.9 ± 1.8	6.2 ± 0.2*

*$p < 0.05$ and **$p < 0.01$ statistically significant difference *versus* control cell line (GM130c).

values of the DKC and the control cells remained constant during the 4 wk (**Table II**). In contrast, the DT markedly increased in DKC cell lines, reaching a value of 416 h in GM3193 at the end of the fourth week; at this time in GM3194, the DT could not be evaluated due to the death of almost all the cells. In the control line, the DT at the end of the fourth week was 20 h.

DISCUSSION

This study demonstrates that the increased DT, which characterizes DKC cell lines, is not related to an alteration of ribosomal biogenesis but to an increase in the cell mortality rate.

The DT was much greater in the DKC cell lines (75 h and 70 h for GM3193 and GM3194, respectively) than in the control line (23 h). This finding is in keeping with previous reports by other authors regarding the slower growth of cells deriving from patients with DKC (Dokal *et al*, 1992).

Our data on ribosomal biogenesis were obtained by [^{3}H]uridine incorporation into nuclear rRNA fractions. The fractions extracted at 50°C and 4°C, respectively, are composed of precursor and mature rRNA molecules. Thus, the technique provides information on the entity of both transcription and maturation of rRNA (Dabeva *et al*, 1978; Derenzini *et al*, 1987). We found that the synthesis of precursor rRNA was greater in DKC cells than in controls. Furthermore, no impairment of the maturation process was evident, as the absolute values of [^{3}H]uridine-labeled mature rRNA were greater in DKC cells than in controls. In addition, the finding that the percentage of [^{3}H]uridine-labeled newly synthesized rRNA molecules in the 4°C fraction was lower in DKC than in controls excludes the possibility of accumulation of ribosomal subunits in the nucleus due to a defect in the transport of mature ribosomal subunits. This set of results was confirmed by morphologic observations showing that nucleolar size is greater in DKC cells than in controls, as evaluated after silver staining, and that the organization of the nucleolar components is typical of highly active nucleoli (very numerous fibrillar centers surrounded by an evident dense fibrillar component) (Derenzini *et al*, 1990).

This demonstration that in DKC cell lines a greater ribosomal biogenesis is associated with a longer DT contrasts with reports indicating that the activity of the nucleolus correlates with cell proliferation rate (Derenzini *et al*, 1998, 2000). This discrepancy was clarified by evaluating the incorporation of [^{3}H]thymidine in the cell lines, standardized for an equal number of alive cells. The results obtained clearly indicated that DKC cells were characterized by a higher proliferative activity than control cells.

In order to explain the slower population DT of DKC cell lines, we considered the possibility that DKC cell lines might be characterized by a greater rate of cell death than control cells. Therefore, we measured the mortality rate of the two DKC cell lines and of the control line over a period of 4 wk both by the Trypan blue exclusion method and by flow cytometric quantification of apoptotic cells. Our results demonstrated that in DKC GM3193 and GM3194 cell lines the mortality rate progressively

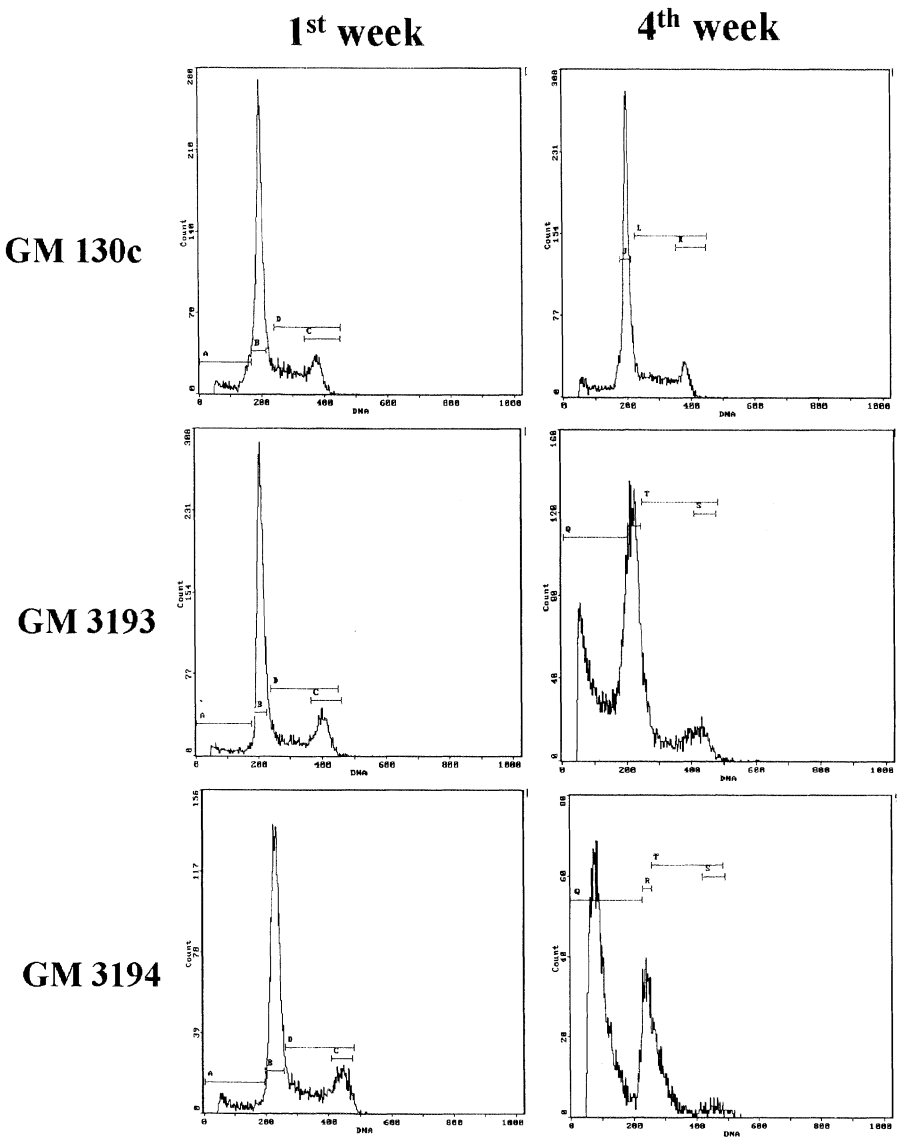

Figure 4. Evaluation of apoptosis over time by flow cytometry. Cytofluorimetric analysis of GM130c (control), GM3193 (DKC), and GM3194 (DKC) cell lines after the first and the fourth week of culture, stained with propidium iodide. In the DKC lines the hypodiploid peak rises remarkably indicating an increase in the number of apoptotic cells.

increased from the first to the fourth week, reaching values of 69% and 95%, respectively, as evaluated by the Trypan blue exclusion test and of 48.7% and 65.4%, respectively, as evaluated by flow cytometry. By contrast, the mortality rate in the control cell line at the fourth week was only 28% as evaluated by Trypan blue staining or 16.2% according to flow cytometry. The discrepancy between Trypan blue staining and flow cytometry values can be explained by the fact that Trypan blue stains all the cells with a damaged membrane, including those without the DNA degradation detected by flow cytometry. Taken together with the finding that [^{3}H]thymidine incorporation was always greater in DKC than in control cells, these data demonstrate that rather than depending on proliferative capacity the longer DT of the DKC cell lines is actually caused by their high mortality rate, which increases progressively as the number of cell cycles increases.

The marked nature of the apoptotic process and its progressive increase over time may be explained by previous observations demonstrating that DKC cells (including the same cell types utilized in this study) are characterized by a lower telomerase activity and shorter telomeres with respect to cells from nonaffected individuals (Mitchell *et al*, 1999). Indeed, as dyskerin is related to the telomerase complex, its alteration in DKC could cause a functional defect and progressive telomere shortening. There is evidence that progressive telomere shortening over successive cell cycles may lead to intense cell death by apoptosis (Herbert *et al*, 1999; Zhang *et al*, 1999).

Our demonstration that, whereas ribosomal biogenesis in DKC is normal, cell growth is curtailed by a dramatic rise in apoptosis related to the number of duplicative cycles can effectively explain the clinical features of DKC. In practice, a constitutive defect in ribosomal biogenesis would impair cell proliferation from the early phases of embryonic development, whereas the alterations of epidermis, mucosae, and bone marrow observed in DKC actually emerge much later (usually after 10 y of age) (Dokal, 1996; Knight *et al*, 1998). By contrast, the severity of the proliferating-tissue defects observed in DKC over time is consistent with our finding that cell death rate increases progressively in relation to the number of cell divisions.

This work was supported by Grants from the Ministero della Ricerca Scientifica e Tecnologica (MURST) 40 and 60%, Pallotti's Legacy for Cancer Research, Regione Emilia Romagna (DGR 4243/1991), the Italian Association for Cancer Research (AIRC, Milan), and University of Bologna (Funds for selected research topics). The authors are grateful to Mr. Robin M.T. Cooke for editing.

REFERENCES

Cadwell C, Yoon HJ, Zebarjadian Y, Carbon J: The yeast nucleolar protein Cbf5p is involved in rRNA biosynthesis and interacts genetically with the rRNA polymerase I transcription factor RRN3. *Mol Cell Biol* 17:6175–6183, 1997

Cole HN, Rauschkolb JC, Toomey J: Dyskeratosis congenita with pimentation, dystrophia unguis and leukokeratosis oris. *Arch Dermatol Syph* 21:71–95, 1930

Dabeva MD, Dudov KP, Hadjialov AA, Stoykova AS: Quantitative analysis of rat liver nucleolar and nucleoplasmic ribosomal ribonucleic acids. *Biochem J* 171:367–374, 1978

Derenzini M, Farabegoli F, Pession A, Novello F: Spatial redistribution of ribosomal chromatin in the fibrillar centres of human circulating lymphocytes after stimulation of transcription. *Exp Cell Res* 170:31–41, 1987

Derenzini M, Thiry M, Goessens G: Ultrastructural cytochemistry of the mammalian cell nucleolus. *J Histochem Cytochem* 38:1237–1256, 1990

Derenzini M, Trerè D, Pession A, Montanaro L, Sirri V, Ochs RL: Nucleolar function and size in cancer cells. *Am J Pathol* 152:1291–1297, 1998

Derenzini M, Trerè D, Pession A, Govoni M, Sirri V, Chieco P: Nucleolar size indicates the rapidity of cell proliferation in cancer tissues. *J Pathol* 191:181–186, 2000

Dokal I: Dyskeratosi congenita: an inherited bone marrow failure syndrome. *Br J Haematol* 92:775–779, 1996

Dokal I, Bungey J, Williamson P, Oscier D, Hows J, Luzzatto L: Dyskeratosis congenita fibroblasts are abnormal and have unbalanced chromosomal rearrangements. *Blood* 80:3090–3096, 1992

Engmann MF: A unique case of reticular pigmentation of the skin with atrophy. *Arch Dermatol Syphil* 13:685–687, 1926

Heiss NS, Knight SW, Vulliamy TJ, *et al*: X-linked dyskeratosis congenita is caused by mutations in a highly conserved gene with putative nucleolar functions. *Nat Genet* 19:32–38, 1998

Heiss NS, Girod A, Salowski R, Wiemann S, Pepperkok R, Poustka A: Dyskerin localizes to the nucleolus and its mislocalization is unlikely to play a role in the pathogenesis of dyskeratosis congenita. *Hum Mol Genet* 8:2515–2524, 1999

Herbert B, Pitts AE, Baker SI, Hamilton SE, Wright WE, Shay JW, Corey DR: Inhibition of human telomerase in immortal human cells leads to progressive telomere shortening and cell death. *Proc Natl Acad Sci USA* 96:14276–142781, 1999

Knight SW, Vulliamy TJ, Copplestone A, Gluckman E, Mason PJ, Dokal I: Dyskeratosis congenita registry: identification of new features of DC. *Br J Haematol* 103:990–996, 1998

Knight SW, Heiss NS, Vulliamy TJ, Greschner S, Stavrides G, Pai GS, Lestringant G, Varma N, Mason PJ: X-linked dyskeratosis congenita is predominantly caused by missense mutations in the *DKC1* gene. *Am J Hum Genet* 65:50–58, 1999

Meier UT, Blobel G: Nopp140 shuttles on tracks between nucleoplasm and cytoplasm. *Cell* 70:127–138, 1992

Meier UT, Blobel G: Nap57, a mammalian nucleolar protein with a putative homolog in yeast and bacteria. *J Cell Biol* 127:1505–1514, 1994

Mitchell JR, Wood E, Collins K: A telomerase component is defective in the human disease dyskeratosis congenita. *Nature* 402:551–555, 1999

Nicoletti L, Migliorati G, Pagliacci MC, Grignani F, Riccardi C: A rapid and simple method for measuring thymocyte apoptosis by propidium iodide staining and flow cytometry. *J Immunol Meth* 139:271–279, 1991

Patterson MK: Measurement of growth and viability of cells in culture. *Meth Enzymol* 58:141–152, 1979

Ploton D, Menager M, Jeannesson P, Himber G, Pigeon F, Adnet JJ: Improvement in the staining and in the visualization of the argyrophilic proteins of the nucleolar organizer region at the optical level. *Histochem J* 18:5–14, 1986

Zhang X, March V, Zhou W, Harrington L, Robinson MO: Telomere shortening and apoptosis in telomerase-inhibited human tumor cells. *Genes Dev* 13:2388–2399, 1999

Zinesser F: Atrophia cutis reticularis cum pigmentatione, dystrophia unguium et leukoplakia oris. *Ikonogr Dermatol (Hyoto)* 5:219–223, 1906